INCREASE OF MASS TRANSPORT LOSS IN POROUS MEDIA CAUSED BY CARBON CORROSION IN PEM FUEL CELLS

Xu Zhang[1, 2], Yupeng Yang[1], Xuyang Zhang[2], Liejin Guo[1], Hongtan Liu[2]
[1] Clean Energy Research Institute, Department of Mechanical and Aerospace Engineering, University of Miami, Coral Gables, FL 33146, USA
[2] International Research Center for Renewable Energy, State Key Laboratory of Multiphase Flow in Power Engineering, Xi'an Jiaotong University, Xi'an, Shaanxi 710049, P R China
Corresponding author: Hongtan Liu, e-mail: hliu@miami.edu (H. Liu).

REFERENCE NO

FCEL-04

Keywords:
Gas diffusion layer, Carbon corrosion, Degradation, Mass transport loss, Proton exchange membrane fuel cell (PEMFC).

ABSTRACT

Identification of the origins of mass transport loss increase caused by carbon corrosion in proton membrane fuel cell (PEMFC) is critical to propose mitigation strategies. However, *in situ* studies of the mass transport process are difficult due to the compact configuration of the single cell. In this study, the increases of mass transport loss are decoupled. The cathode GDL in the aged cell is substituted with a fresh GDL. Meanwhile, the cathode GDL in an activated cell is also substituted with the aged GDL. Polarization curve and electrochemical impedance spectroscopy (EIS) measurement are conducted. Although the kinetic degradation accounts for the primary decay, the increase of mass transport loss is so significant that in some conditions cell performance would be greatly limited by the mass transport loss. The CL is the primary contributor to increase of mass transport loss. Besides, the aged GDL also tends to retain more water which would increase the mass transport loss under high RH conditions.

1. INTRODUCTION

Mass transport in carbon-based porous layers is essential to the performance of the proton exchange membrane fuel cell (PEMFC) [1, 2]. Supply of gaseous reactant to reaction sites at catalyst layer (CL) though gas diffusion layer (GDL) and micro porous layer (MPL), and effective management of water balance in the porous components ensure the continuous reaction in CL and negligible mass transport loss [3, 4]. However, currently the most commonly used porous components are carbon-based and cannot be avoided to undergo severe corrosion conditions, under which high electrode interfacial potential is created due to either frequent start-up/shut-down cycling, reactant starvation or water flooding [5-7]. Besides well-documented kinetics degradation due to the corrosion of the catalyst support in CL, another important concern of the carbon corrosion is the deterioration of mass transport process inside the porous components [8, 9]. The gaseous transport and water management inside the porous components, including CL, GDL and MPL, can be severely damaged when carbon corrosion occurs under high electrode potential [10, 11].

Corrosion of carbon support to catalyst particle in CL leads to collapse of the pore space and obstructs the oxygen transport pathways [12]. The interconnected network of the carbon particles was found to be severely damaged, creating isolated pores, unfavourable pore size distribution, and embedded platinum particles [13, 14]. The access of the oxygen to the catalyst particles thus is limited, which decrease the utilization of the catalyst and be also responsible for severe mass transport loss [14]. Another result of carbon corrosion is the creation of a more hydrophilic surface due to formation of diverse carbon oxide groups and increase of the surface roughness (structural defects) [15]. The water balance inside the CL pore space would be affected and the propensity of flooding increases substantially [16, 17]. Since the mass transport resistance in CL accounts for a significant loss of performance, both the increase of gaseous diffusion resistance and deterioration of water management caused by carbon corrosion lead

to great increase of mass transport loss in polarization curve[18, 19].

The carbon corrosion also occurs in GDL and MPL, and further affects the water balance in porous layers [20-22]. GDL are often carbon-fibre based paper or cloth with polytetrafluoroethylene (PTFE) wet-proofed to enhance the water management capability. A fine MPL, a porous layer of carbon powder impregnated with PTFE particles, is often inserted between CL and GDL to improve the water management [7, 23]. Park *et al* [20] reviewed the durability and degradation issues of the GDL in PEMFC. The chemical/electrochemical degradation is primary causes for water deterioration in GDL and MPL. Carbon corrosion cause severe structure damages to GDL and consequently increases in contact resistance and water flooding. Yu *et al* [11] studied the hydrophobicity loss of GDL caused by electrochemical corrosion. The decrease of hydrophobicity of GDL are associated to the loss of carbon material and PTFE. Ha *et al* [24] also investigated the carbon corrosion at the GDL and found that the carbon component of the GDL is easily corroded while PTFE component doesn't be affected by electric potential very much. Damages of GDL pore structure and hydrophobicity loss jeopardize the water removal ability and renders the increase of mass transport loss. The corrosion of MPL is even severe as it locates close proximity to the CL [9]. In this scenario, homogeneous PTFE coating to GDL/MPL is proposed to be an effective way to suppress the oxidation of the carbon material [25].

Since the achievement of good performance and degradation of the cell components are interactive processes that occurs simultaneously, the discriminations of aforementioned increases of the mass transport loss are difficult. It is presumed that the most severe corrosion occurs in CL due to highest electrode potential and the catalytic effect of platinum[26, 27]. However, the MPL and GDL also cannot be avoided from such degradation mechanism. Spernjak *et al* [28] found that the present of MPL can effectively alleviate the carbon corrosion in CL, although overall CO_2 release increase due to corrosion occurred in MPL itself. Furthermore, the accumulation and transport of liquid water inside the porous components, which are important causes to the excursive electrode interfacial potential and reactant for corrosion reaction, are in quite sophisticated balance [29, 30]. Malfunction of water management exacerbates the material degradation [31, 32]. Hence, understanding of the degradation of a stand-along component contributes little to the understanding of the overall performance. The origin of mass transport deterioration in each porous layer should be carefully clarified.

As stated above, carbon corrosion causes severe pore structure damages and hydrophobicity loss to porous layers in a PEMFC. The increase of mass transport loss has been widely reported. However, due to the multi-layered configuration and compact assembly of the porous layers in an as-received electrode/cell, a breakdown of mass transport losses in each layer is difficult, which makes the pertinent mitigation strategies impossible. Hence, in this work, experiments are conducted to investigate the origin of the mass transport loss increase in a single cell using an accelerated stress test (AST) for carbon corrosion. To discriminate the mass transport resistance in CL and GDL, the cell performance is characterized under different relative humidity (RH). The mass transport processes are analysed by polarization curves and electrochemical impedance spectroscopy (EIS).

2. EXPERIMENTAL

2.1. Experimental system

A Nafion-212 based membrane electrode assembly (MEA, Pearl Hydrogen Power Source) is used. Platinum loading on both sides are is 0.4 $mg \cdot cm^{-2}$. The active area of the electrode is 16 cm^2, controlled by gaskets on both sides. The MEA is sandwiched between two carbon papers (Toray 060, Toray Industries. Inc., Japan). The MEA, GDLs and gaskets are assembled by a single cell testing hardware with graphite bipolar plates curved with single serpentine flow field. The depth of channel is 1 mm and the widths of channel

and land are 2 mm. The reactant flows are in co-flow. The single cell is connected to a fuel cell testing station (FCTS-16, Fuel Cell Technologies.Inc., USA) for operating conditions controlling and a potentiostat/galvanostat (HCP-803, Bio-Logic, Inc., France) for electrochemical characterization.

2.2. Cell conditioning and performance characterization

Prior to the performance characterizations, the cell is conditioned by scanning the voltage between open circuit voltage and 0.2 V with 0.05 V increment every 5 minutes. During conditioning, the cell is maintained at 343 K and atmospheric pressure with fully humidified hydrogen and air with stoichiometries at 1.5 and 2 corresponding to 1 A cm^{-2}, respectively. The cycling continues until a stall performance has been reached. Then the polarization curve and EIS measurement are conducted at the beginning of life (BOL). The polarization curves are obtained by sweeping the voltage from OCV to 0.2 V at a rate of 1 mV s^{-1}. EISs are measured at different current densities and air RHs to identify the different resistances.

After the initial characterization, a high potential holding protocols, i.e.,1.4 V, is employed as the AST condition to mimic the carbon corrosion in fuel cell. Fully saturated hydrogen and nitrogen with flow rates of 200 sccm are purged at anode and cathode during the AST, respectively. The AST lasts for 15 h. After AST, a performance recovery procedure is performed prior to the performance characterization to recover the reversible degradation accumulated during the ASTs [33]. The recovery procedure has same protocol with the conditioning process. Then, the characterizations are performed under the same conditions as those used at BOL.

To discriminate the mass transport resistances resulted from CL and GDL, the aged cell is disassembled gently and then the aged cathode GDL can be extracted easily due to slight small clamping pressure used (6 N m). The aged GDL is then assembled into an activated single cell with identical components. Effects of the aged GDL on the performance of the activated cell are characterized. Similarly, the extracted GDL from the activated cell is assembled into the aged cell, and its effect is measured. Only difference between two cells compared are the cathode GDL. The CCM, anode GDL and other components are all from the same cell. The disassembly and assembly are repeated for several times and the repeatability is guaranteed. The procedure of the experiment is shown schematically in Fig 1.

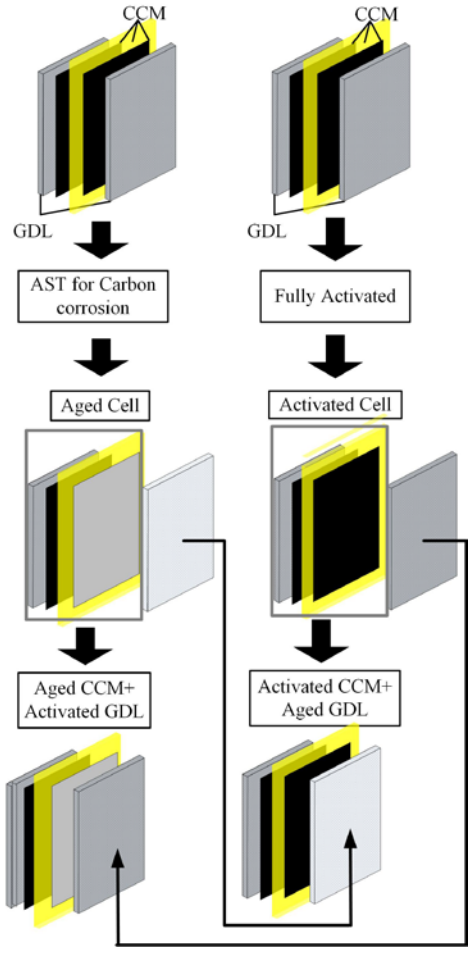

Fig. 1. Experimental procedure to discriminate the mass transport loss in cathode GDL and CL.

3. RESULTS AND DISCUSSION

3.1. Performance degradation

The degradation of cell performance is recorded firstly. To analyse the mass transport loss, cell performance is characterized under different air RH, i.e., 50% and 75%. Effects of water content on the mass transport loss could be classified. Figure 2 shows the polarization

curves before and after degradation test with air RH at 50%. At BOL, the cell only shows slight mass transport loss when current density exceeds 700 mA cm^{-2}. The mass transport loss become apparent even with current density exceeding 500 mA cm^{-2} after degradation test. EISs are measured before and after degradation test as shown in Fig. 3 (a). The results are fitted with an equivalent circuit (R(RQ)(RQ)) to decouple the high frequency resistance (HFR), the charge transfer resistance and the mass transfer resistance, as shown in table in Fig 3. (a) and Fig 3. (b). Constant phase elements (CPEs) rather than pure capacitances are used to account for the processes in porous electrode. At 500 mA cm^{-2}, the mass transport resistance increases from 0.243 ohm cm^2 to 1.03 ohm cm^2, with 4-fold increase.

HFRs and charges transfer resistances are also obtained and exhibits substantial increases. Under smaller current density, i.e., 150 mA cm^{-2}, which water effect is supressed, the effect of mass transport diminishes. HFR increases from 0.22 ohm cm^2 to 0.256 ohm cm^2. HFR remains unchanged under 500 mA cm^{-2} due to increased water production. The charge transfer resistance presents substantial increases from 0.508 ohm cm^2 to 0.843 ohm cm^2 at 150 mA cm^{-2}, and 0.237 ohm cm^2 to 0.642 ohm cm^2 at 500 mA cm^{-2}, respectively. As a result, the increases of ohmic loss, activation loss and mass transport loss lead to severe performance degradation.

Polarization curves at elevated air RH exhibit significant mass transport loss before and after degradation test, as shown in Fig. 4. The water content in the porous layers increases under higher RH conditions, leading to larger resistance to the gaseous reactant diffusion. Besides, EIS data presented in Fig. 5 indicates that the increase of mass transport resistance is up to 10-fold after degradation test. The carbon corrosion makes the cell performance be severely affected by water accumulation, even flooding.

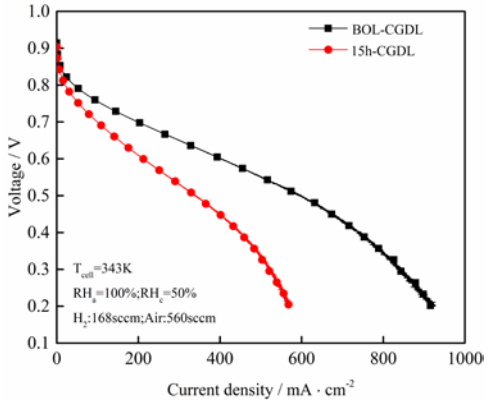

Fig. 2. Polarization curves before and after AST under 50% cathode RH condition.

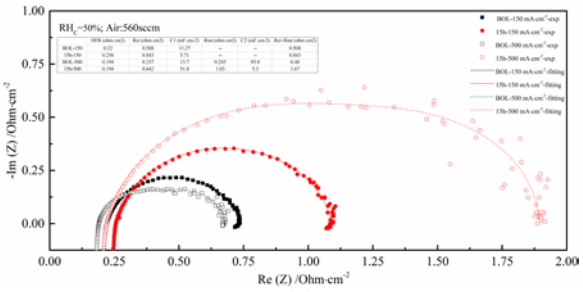

(a)

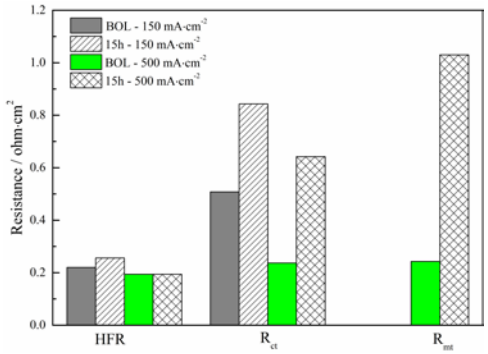

(b)

Fig. 3. EISs measured before and after AST with air RH at 50%, (a) EISs and fitting and (b) fitted resistances under low RH condition.

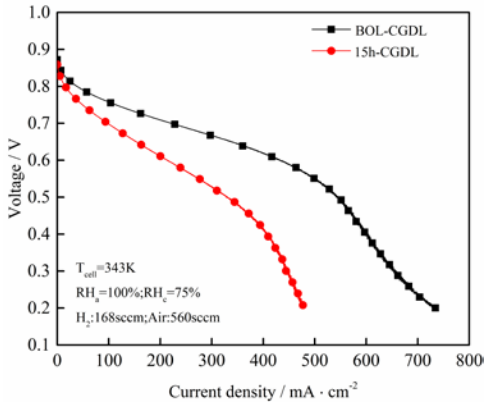

Fig. 4. Polarization curves before and after AST under 75% cathode RH condition.

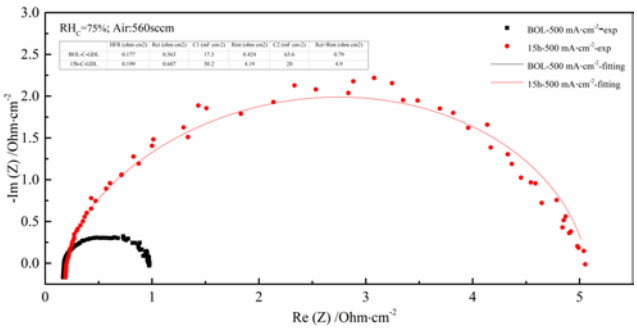

Fig. 5. EISs measured before and after AST with air RH at 75%.

3.2. Effects of activated GDL on the performance of the aged cell

To clarify the origin of the mass transport loss increase, the specialized experiment is carried out as shown Fig. 1. Firstly, the cathode GDL in the aged cell is substituted by a GDL extracted from the activated cell. Then the cell performance is compared between the aged and activated cathode GDL.

Figure 6 shows the changes of polarization curve when the aged GDL is substituted by the activated GDL. Under low air RH condition, the substitution doesn't give rise to apparent performance improvement as shown in Fig. 6 (a). Since the effect of water content is suppressed under low RH condition, the cell performance is nearly independent on the mass transport loss. The primary performance degradation under low RH condition (Fig. 2) should be caused by the degradation in CL and increase of ohmic resistance. By increasing RH to 75% as shown in Fig 6(b), apparent improvement is observed at large current density region with activated GDL, indicating severe water accumulation arising from the aged GDL. The high voltage holding used as AST protocol in this study causes material physicochemical properties degradation (hydrophobicity loss) and microstructure damages in GDL. Therefore, the water management of GDL is deteriorated due to the carbon corrosion. Besides, by comparing the performance under low and high RH condition, it is presumed that the reactant diffusion in GDL is not affected by carbon corrosion.

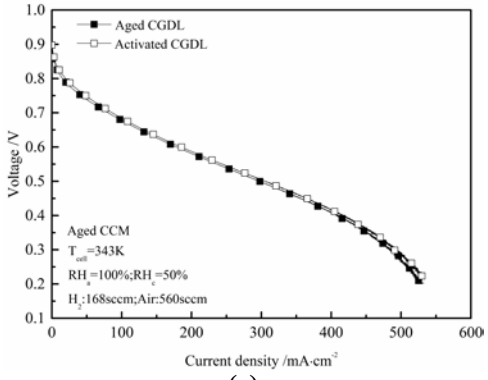

(a)

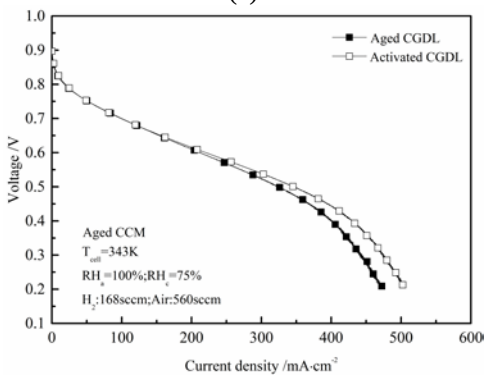

(b)

Fig. 6. Polarization curves of single cells based on aged CCM, with aged GDL and activated GDL under (a) 50% cathode RH condition and (b) under 75% cathode RH condition.

EISs are also measured to confirm the mass transport loss caused by the aged GDL. EIS is firstly measured at small current density under low air RH condition as shown in Fig 7. (a). The spectra with activated GDL coincides with this with the aged GDL. It means that the substitution of the cathode GDL and several assembly/disassembly cycles don't affect other components and the consistent of performance measurement.

EISs measured at larger current density and elevated air RH condition confirm that the aged GDL has larger mass transport resistance, as shown in Fig. 7 (b). Even when the air RH is 50%, the aged GDL still has larger mass transport resistance due to more water generation at 400 mA cm^{-2}. By increasing the air RH from 50% to 75%, the difference is more apparent. The water management capability of the aged GDL is severely deteriorated, making the propensity of flooding increase.

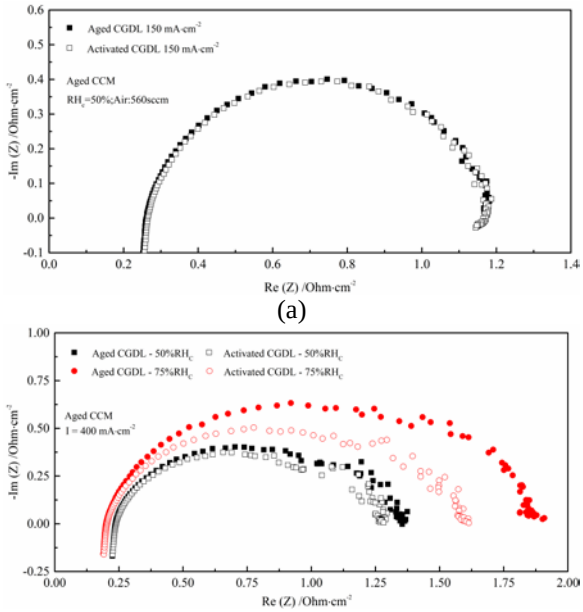

Fig. 7. EISs measured with aged GDL and activated GDL, at (a) 150 mA cm^{-2} and 50% cathode RH condition, (b) large current density.

The substitution of the aged GDL with activated GDL doesn't recover the cell degradation even under high current density and high RH condition. It indicates the major performance loss induced by carbon corrosion should be caused by the degradation in cathode CL, including both kinetic degradation and mass transport loss increase. The aged GDL also contributes to the increase of mass transport loss due to the deterioration of water management. Besides, it is presumed that the deterioration of water management in cathode CL should be more severe due to its even harsher condition.

3.3. Effects of aged GDL on the performance of the activated cell

Next the aged cathode GDL extracted from the aged cell is used to substitute the activated cathode GDL of the activated cell. Effects of the aged GDL on the performance of the activated cell are studied. Interestingly, the cell with aged cathode GDL has better performance under low air RH condition, as shown in Fig. 8 (a). Since the aged GDL tends to retain more liquid water due to reduction of hydrophobicity and pore structure caused by carbon corrosion, the water content increases due to the water-retaining property of the aged GDL when it is assembled into the activated cell. Under low humidity, this benefits membrane hydration and thus low ohmic resistance. From Fig. 8 (a), it is apparent that the slope of polarization curve is smaller in cell with aged cathode GDL while no obvious mass transport limitation is observed. However, when the air RH is increased, as shown in Fig. 8 (b), apparent mass transport loss appears with current density exceeding 500 mA cm^{-2}, caused by more water content retained by the aged cathode GDL.

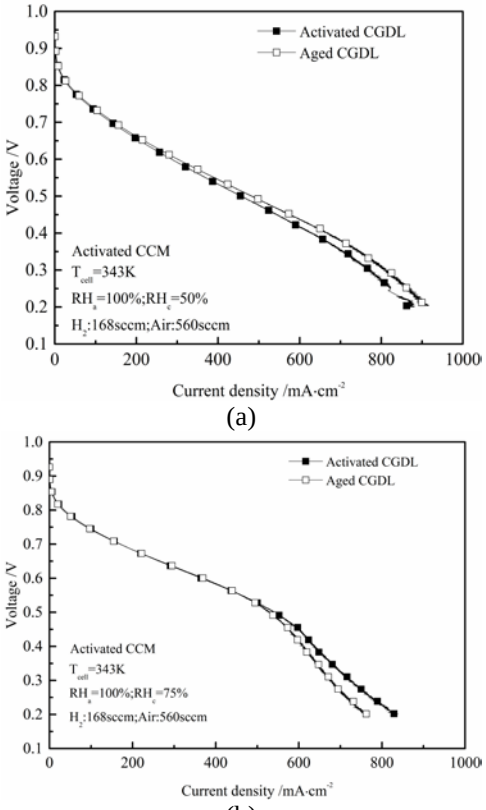

Fig. 8. Polarization curves of single cells based on activated CCM, with aged GDL and activated GDL under (a) 50% cathode RH condition and (b) under 75% cathode RH condition.

EISs are conducted to substantiate above results. Figure 9 (a) shows impedance spectra for activated cathode GDL and aged cathode GDL under low air RH and small current density. The cell with aged cell gives rise to apparent smaller ohmic resistance. Besides, the charge transfer resistances are nearly same, indicating that the substitution doesn't affect the ORR kinetic in CL. These are consistent to the results from polarization curves. Moreover, though the air RH is low, the EISs at larger current densities, e.g., 500 mA cm^{-2} and 750

mA cm^{-2} in Fig. 9 (b), still show slight increases in mass transport resistance.

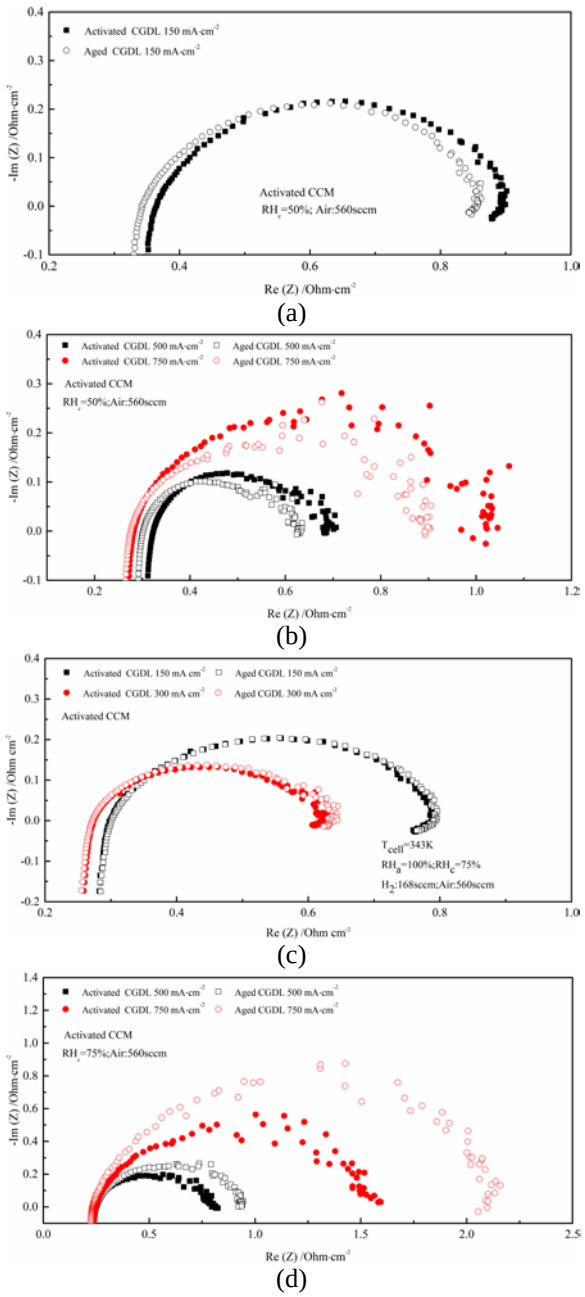

Fig. 9. EISs measured with aged GDL and activated GDL, at (a) small current density and 50% cathode RH, (b) large current density and 50% cathode RH, (c) small current density and 75% cathode RH, (b) large current density and 75% cathode RH.

When the air RH increases to 75%, the better membrane hydration diminishes the effect of the substitution of the cathode GDL on ohmic resistance, as shown in Fig. 9 (c). The EISs spectra nearly overlaps at small current density. With further increase of current density shown in Fig. 9 (d), the mass transport resistances with the aged GDL are apparently larger than those with the activated GDL.

4. CONCLUSIONS

In this study, the increase of mass transport in porous layers in a single PEMFC caused by an accelerated stress test is discriminated. In order to decouple increase of the mass transport loss in cathode CL and GDL, a specialized experiment is conducted and the contributions of the CL and GDL on the mass transport loss increase are studied. The following conclusions can be obtained from this study:

- The increase of mass transport resistance and kinetic degradation in CL contributes to major performance degradation.
- Increase of mass transport loss is significant under certain conditions.
- Aged GDL tends to retain more liquid water due to deterioration of water management caused by carbon corrosion.
- The increase of mass transport loss is more obvious at larger current density region and high RH condition.

Acknowledgements

The financial supports from Chang Jiang Scholars Program of Ministry of Education of China, and the National Science Foundation of China for Creative Research Groups (No. 51121092) are gratefully acknowledged.

References

1. Weber, A.Z., et al., *A Critical Review of Modeling Transport Phenomena in Polymer-Electrolyte Fuel Cells.* Journal of the Electrochemical Society, 2014. **161**(12): p. F1254-F1299.
2. Banerjee, R. and S.G. Kandlikar, *Two-phase flow and thermal transients in proton exchange membrane fuel cells - A critical review.* International Journal of Hydrogen Energy, 2015. **40**(10): p. 3990-4010.
3. Jiao, K. and X.G. Li, *Water transport in polymer electrolyte membrane fuel cells.* Progress in Energy and Combustion Science, 2011. **37**(3): p. 221-291.

4. Li, H., et al., *A review of water flooding issues in the proton exchange membrane fuel cell.* Journal of Power Sources, 2008. **178**(1): p. 103-117.
5. Yousfi-Steiner, N., et al., *A review on polymer electrolyte membrane fuel cell catalyst degradation and starvation issues: Causes, consequences and diagnostic for mitigation.* Journal of Power Sources, 2009. **194**(1): p. 130-145.
6. Borup, R., et al., *Scientific aspects of polymer electrolyte fuel cell durability and degradation.* Chem Rev, 2007. **107**(10): p. 3904-51.
7. de Bruijn, F.A., V.A.T. Dam, and G.J.M. Janssen, *Review: Durability and Degradation Issues of PEM Fuel Cell Components.* Fuel Cells, 2008. **8**(1): p. 3-22.
8. Hitchcock, A.P., et al., *Carbon corrosion of proton exchange membrane fuel cell catalyst layers studied by scanning transmission X-ray microscopy.* Journal of Power Sources, 2014. **266**(0): p. 66-78.
9. Spernjak, D., et al., *Characterization of Carbon Corrosion in a Segmented PEM Fuel Cell.* Polymer Electrolyte Fuel Cells 11, 2011. **41**(1): p. 741-750.
10. Fairweather, J.D., et al., *Effects of Cathode Corrosion on Through-Plane Water Transport in Proton Exchange Membrane Fuel Cells.* Journal of the Electrochemical Society, 2013. **160**(9): p. F980-F993.
11. Yu, S.C., et al., *Study on hydrophobicity loss of the gas diffusion layer in PEMFCs by electrochemical oxidation.* Rsc Advances, 2014. **4**(8): p. 3852-3856.
12. Star, A.G. and T.F. Fuller, *FIB-SEM Tomography Connects Microstructure to Corrosion-Induced Performance Loss in PEMFC Cathodes.* Journal of the Electrochemical Society, 2017. **164**(9): p. F901-F907.
13. Schulenburg, H., et al., *3D Imaging of Catalyst Support Corrosion in Polymer Electrolyte Fuel Cells.* Journal of Physical Chemistry C, 2011. **115**(29): p. 14236-14243.
14. Star, A.G. and T.F. Fuller, *FIB+SEM Tomography and Numerical Simulation of Corroded PEM Fuel Cell Cathodes.* ECS Transactions, 2015. **69**(17): p. 431-441.
15. Castanheira, L., et al., *Carbon Corrosion in Proton-Exchange Membrane Fuel Cells: From Model Experiments to Real-Life Operation in Membrane Electrode Assemblies.* Acs Catalysis, 2014. **4**(7): p. 2258-2267.
16. Kim, M., et al., *Effects of anode flooding on the performance degradation of polymer electrolyte membrane fuel cells.* Journal of Power Sources, 2014. **266**: p. 332-340.
17. Chen, J.X., J.W. Hu, and J.R. Waldecker, *A Comprehensive Model for Carbon Corrosion during Fuel Cell Start-Up.* Journal of the Electrochemical Society, 2015. **162**(8): p. F878-F889.
18. Ghosh, S., et al., *In-plane and through-plane non-uniform carbon corrosion of polymer electrolyte fuel cell cathode catalyst layer during extended potential cycles.* Journal of Power Sources, 2017. **362**: p. 291-298.
19. Zhang, Y.L., et al., *Study of the degradation mechanisms of carbon-supported platinum fuel cells catalyst via different accelerated stress test.* Journal of Power Sources, 2015. **273**: p. 62-69.
20. Park, J., et al., *A review of the gas diffusion layer in proton exchange membrane fuel cells: Durability and degradation.* Applied Energy, 2015. **155**: p. 866-880.
21. Dubau, L., et al., *A review of PEM fuel cell durability: materials degradation, local heterogeneities of aging and possible mitigation strategies.* Wiley Interdisciplinary Reviews-Energy and Environment, 2014. **3**(6): p. 540-560.
22. Ous, T. and C. Arcoumanis, *Degradation aspects of water formation and transport in Proton Exchange Membrane Fuel Cell: A review.* Journal of Power Sources, 2013. **240**(0): p. 558-582.
23. Park, S., J.W. Lee, and B.N. Popov, *A review of gas diffusion layer in PEM fuel cells: Materials and designs.* International

Journal of Hydrogen Energy, 2012. **37**(7): p. 5850-5865.
24. Ha, T., et al., *Experimental study on carbon corrosion of the gas diffusion layer in polymer electrolyte membrane fuel cells.* International Journal of Hydrogen Energy, 2011. **36**(19): p. 12436-12443.
25. Hiramitsu, Y., et al., *Controlling gas diffusion layer oxidation by homogeneous hydrophobic coating for polymer electrolyte fuel cells.* Journal of Power Sources, 2011. **196**(13): p. 5453-5469.
26. Owejan, J.P., J.E. Owejan, and W.B. Gu, *Impact of Platinum Loading and Catalyst Layer Structure on PEMFC Performance.* Journal of the Electrochemical Society, 2013. **160**(8): p. F824-F833.
27. Speder, J., et al., *On the influence of the Pt to carbon ratio on the degradation of high surface area carbon supported PEM fuel cell electrocatalysts.* Electrochemistry Communications, 2013. **34**: p. 153-156.
28. Spernjak, D., et al., *Influence of the microporous layer on carbon corrosion in the catalyst layer of a polymer electrolyte membrane fuel cell.* Journal of Power Sources, 2012. **214**: p. 386-398.
29. Dubau, L., et al., *Evidences of "Through-Plane" Heterogeneities of Aging in a Proton-Exchange Membrane Fuel Cell.* Ecs Electrochemistry Letters, 2012. **1**(2): p. F13-F15.
30. Ettingshausen, F., et al., *Spatially resolved degradation effects in membrane-electrode-assemblies of vehicle aged polymer electrolyte membrane fuel cell stacks.* Journal of Power Sources, 2009. **194**(2): p. 899-907.
31. Wang, X.F., et al., *Impact of In-Cell Water Management on the Endurance of Polymer Electrolyte Membrane Fuel Cells.* Journal of the Electrochemical Society, 2014. **161**(6): p. F761-F769.
32. Kandlikar, S.G., M.L. Garofalo, and Z. Lu, *Water Management in A PEMFC: Water Transport Mechanism and Material Degradation in Gas Diffusion Layers.* Fuel Cells, 2011. **11**(6): p. 814-823.